[Tris(pyrazolyl)borato]vanadium(III) Phosphates: Structural Motifs from the Extended Solid and Models for the Interaction with DNA

Norman S. Dean,[1a] Ladd M. Mokry,[1a] Marcus R. Bond,[1a,c] C. J. O'Connor,[1b] and Carl J. Carrano*,[1a]

Departments of Chemistry, Southwest Texas State University, San Marcos, Texas 78666, and University of New Orleans, New Orleans, Louisiana 70148

Received November 10, 1995[⊗]

The syntheses of five mixed ligand vanadium(III) phosphate/phosphonate complexes are described: dinuclear **I**, $[LVCl\{\mu\text{-}(PhO)_2PO_2\}]_2$; **II**, $[LVCl\{\mu\text{-}Ph_2PO_2\}]_2$; and **III**, $[LVCl\{\mu\text{-}PhP(H)O_2\}]_2$; along with mononuclear **IV**, $[LV\{(PhO)_2POS\}_2DMF]$; and **V**, $[LV\{(PhO)_2PO_2\}]_2{\cdot}H_2O$ where L = hydrotris(pyrazolyl)borate. X-ray crystal structure analysis of **I**, **II**, **IV**, and **V** gave the following parameters: **I**, $C_{12}H_{40}B_2Cl_2N_{12}O_8P_2V_2$, $P\bar{1}$, $a = 9.949(4)$Å, $b = 11.732(4)$ Å, $c = 12.729(3)$ Å, $\alpha = 110.37(1)°$, $\beta = 106.78(1)°$, $\gamma = 104.36(1)°$, $Z = 1$, $V = 1228.8(7)$ Å^3; **II**, $C_{46}H_{98}B_2Cl_{10}N_{12}O_4P_2V_2$, $P\bar{1}$, $a = 11.801(2)$ Å, $b = 12.086(1)$ Å, $c = 12.955(2)$ Å, $\alpha = 81.99(1)°$, $\beta = 65.51(1)°$, $\gamma = 62.60(1)°$, $Z = 1$, $V = 1491.1(5)$ Å^3; **IV**, $C_{36}H_{37}BN_7O_7P_2S_2V$, $P\bar{1}$, $a = 11.003(2)$ Å, $b = 11.816(2)$ Å, $c = 17.167(5)$ Å, $\alpha = 98.68(2)°$, $\beta = 101.81(2)°$, $\gamma = 102.59(2)°$, $Z = 2$, $V = 2087.0(6)$ Å^3; **V**, $C_{69.5}H_{65}B_2N_{15}O_8P_4V_2$, $C2/c$, $a = 12.360(2)$ Å, $b = 26.362(4)$ Å, $c = 23.254(2)$ Å, $\beta = 91.24(8)°$, $Z = 4$, $V = 7575(2)$ Å^3. Magnetic measurements indicate little or no interaction between the V(III) ions in **II** but a modest antiferromagnetic coupling in **I**. These complexes should be good models for the possible modes of bonding between V(III) and biological phosphates such as DNA as well as provide insight into one of the common structural motifs present in vanadium(III) phosphate solid state materials.

Introduction

For some time we have been interested in vanadium phosphate interactions from both a biological and a materials science perspective.[2−4] Vanadium phosphates have received most of their attention from the unusual properties that they can exhibit in the extended solid, and these materials have applications ranging from functioning as size selective inorganic hosts[5] to serving as oxidation catalysts.[6] Much work and many novel vanadium phosphate materials have been developed over the last several years using template-based hydrothermal techniques.[7−10] However, despite the development of these self-assembly methods the more straightforward approach of rationally synthesizing small molecular building blocks which can be used as precursors for the formation of higher order structures under conventional conditions has lagged. In addition, complexes derived from hydrothermal techniques do not suitably address the types of vanadium phosphate interactions that are likely to be present in biological systems. Since much of the work in our laboratory concerns the biological role of vanadium, it is in this latter area that we first became interested in vanadium phosphate chemistry specifically in regard to the interaction of vanadium complexes with DNA.

The interaction of metal ion complexes with simple nucleotides and their polymers, i.e., DNA and RNA, to form ternary complexes has been of some considerable interest either with respect to the action of enzymes which use nucleotides as substrates or in relation to the design of inorganic-based artificial restriction enzymes or anticancer drugs.[11] Besides the well-studied interactions with the metal binding sites of the nucleoside bases (e.g., N7 of guanine) the phosphate groups themselves present potential binding sites. Indeed the antitumor agent Cp_2VCl_2 is thought to react with DNA by some sort of interaction with the phosphate oxygens.[12] Marks et al. have shown that this interaction could be as simple as hydrogen bonding and has reported the crystal structure of the $Cp_2V(H_2O)_2$ diphenyl phosphate adduct.[13] Numerous authors have reported other solution studies of the interaction of V(III) and V(IV) complexes with DNA constituents and concluded that phosphate oxygens were the likely binding sites but no solid structural data have been forthcoming.[14−17] Finally we and others have also shown that a number of V(III) phenanthroline complexes also interact strongly with DNA leading to its facile cleavage.[18]

Together, all of these interests prompted us to prepare a number of LV(III) complexes (L = hydrotris(pyrazolyl)borate)

⊗ Abstract published in *Advance ACS Abstracts,* April 15, 1996.

(1) (1) (a) Southwest Texas State University. (b) University of New Orleans. (c) Present address: Department of Chemistry, Southeast Missouri State University, Cape Girardeau, MO 63701.
(2) Mokry, L. M.; Thompson, J.; Bond, M. R.; Otieno, T.; Mohan, M.; Carrano, C. J. *Inorg. Chem.* **1994**, *33*, 2705.
(3) Otieno, T.; Mokry, L.; Bond, M. R.; Carrano, C. J.; Dean, N. S. *Inorg. Chem*., in press.
(4) Bond, M. R.; Mokry, L.; Otieno, T.; Thompson, J.; Carrano, C. J. *Inorg. Chem*. **1995**, *34*, 1894.
(5) Johnson, D. C.; Jacobson, A. J.; Butler, W. M.; Rosenthal, S. E.; Brody, J. F.; Lewandowski, J. T. *J. Am. Chem. Soc*. **1989**, *111*, 381.
(6) Centi, G.; Trifiro, F.; Edner, J. R.; Francetti, V. M. *Chem. Rev*. **1988**, *88*, 55.
(7) Soghomonian, V.; Haushalter, R. C.' Chen, Q.; Zubieta, J. *Inorg. Chem*. **1994**, *33*, 700.
(8) Huan, G.; Day, V. W.; Jacobson, A. J.; Goshorn, D. P. *J. Am. Chem. Soc*. **1991**, *113*, 3188.
(9) Chen, Q.; Zubieta, J. *Angew. Chem., Int. Ed. Engl*. **1993**, *32*, 261.
(10) Khan, M. I.; Lee, Y.; O'Connor, C. J.; Haushalter, R. C.; Zubieta, J. *Inorg. Chem*. **1994**, *33*, 3855.
(11) Pyle, A. M.; Barton, J. K. In *Progress in Inorganic Chemistry: Bioinorganic Chemistry*; Wiley and Sons Inc.: New York, 1990; Vol. 38.
(12) Toney, J. H.; Marks, T. J. *J. Am. Chem. Soc*. **1985**, *107*, 947.
(13) Toney, J. H.; Brock, C. P.; Marks, T. J. *J. Am. Chem. Soc*. **1986**, *108*, 7263.
(14) Williams, P. H. M.; Baran, E. J. *J. Inorg. Biochem*. **1993**, *50*, 101.
(15) Baran, E. J. In *Metal Ions in Biological Systems*; Sigel, H., Sigel, A., Eds.; Marcel Dekker, Inc.: New York, 1995; Vol. 31.
(16) Katsaros, N. *Trans. Met. Chem*. **1982**, *7*, 72.
(17) Mustafi, D.; Telser, J.; Makinen, M. W. *J. Am. Chem. Soc*. **1992**, *114*, 6219.

S0020-1669(95)01455-8 CCC: $12.00

Table 1. Crystallographic Data and Data Collection Parameters for **I**−**IV**

parameter	**I**	**II**	**IV**	**V**
formula	$C_{12}H_{40}B_2Cl_2N_{12}O_8P_2V_2$	$C_{46}H_{98}B_2Cl_{10}N_{12}O_4P_2V_2$	$C_{36}H_{37}BN_7O_7P_2S_2V$	$C_{69.5}H_{65}B_2N_{15}O_8P_4V_2$
space group	*P*1	*P*1	*P*1	*C*2/*c*
temp, K	298	173	298	223
a, Å	9.949(4)	11.801(2)	11.003(2)	12.360(2)
b, Å	11.732(4)	12.086(1)	11.816(2)	26.362(4)
c, Å	12.729(3)	12.955(2)	17.167(5)	23.254(2)
α, deg	110.37(1)	81.99(1)	98.68(2)	90.00
β, deg	106.78(1)	65.51(1)	101.81	91.24(8)
γ, deg	104.36(1)	62.60(1)	102.59(2)	90.00
V, Å^3	1228.8(7)	1491.1(5)	2087.0(6)	7575(2)
ρ_{calc}, g cm^{-3}	1.483	1.530	1.380	1.438
Z	1	1	2	4
fw	1097.2	1872.9	867.5	819.9
cryst size, mm	0.4 × 0.4 × 0.8	0.5 × 0.4 × 0.1	0.3 × 0.5 × 0.1	0.6 × 0.4 × 0.8
μ, cm^{-1}	0.618	0.868	0.469	0.410
radiation	graphite-monochromated Mo Kα (λ = 0.710 73)			
scan type	ω	$\theta-2\theta$	$\theta-2\theta$	ω
data collection range, deg	3.5−45	3.5−45	3.5−40	3.5−43
R_{merge}, %	1.86	4.6	1.1	1.9
no. unique data	2995	3760	3865	4339
no. obs data, $F > 4.0\sigma(F)$	1935	3043	2098	3800
data:param ratio	6.1:1	8.6:1	4.2:1	6.8:1
transm	0.77/0.91	XABS	0.81/0.85	n/a
R^a	4.99	6.43	6.40	4.82
$R_w{}^a$	5.79	8.32	6.40	4.82
max diff peak, e/Å^3	0.30	1.03	0.33	0.29
Δ/σ(max)	0.000	0.000	0.011	0.649

[a] Quantity minimized $\sum w(F_o - F_c)^2$. $R = \sum|F_o - F_c|/\sum F_o$. $R_w = (\sum w(F_o - F_c)^2/\sum(wF_o)^2)^{1/2}$.

containing phosphate mono- and diesters both to learn more about vanadium phosphate interactions that might occur in biological systems and to investigate their utility as precursors in the rational synthesis of solid state materials. Since the tris(pyrazolyl)borate group is frequently viewed as an inorganic analog to the ubiquitous organometallic ligand Cp, the results of this study should also be applicable to an understanding of the possible modes of interaction of Cp_2VCl_2 with DNA.[19] In this work we examine the structure and properties of a series of mono- and dinuclear LV(III) complexes in which the phosphate groups are terminal and bridging, respectively. Besides providing information about possible bonding modes, the binuclear complexes also serve as models for one of the fundamental building blocks in V(III) phosphate solids. We therefore examine the geometrical conformation of the bridging unit and its role in propagating magnetic exchange and compare these properties to those of the structurally analogous vanadyl complexes.

Experimental Section

Materials. All synthetic procedures were carried out under an atmosphere of pure dry argon or nitrogen by utilizing standard Schlenk techniques. Subsequent workup was carried out in air unless otherwise noted. Solvents were distilled under nitrogen from the appropriate drying agents (CaH_2 or Na/benzophenone). DMF was Burdick and Jackson "distilled in glass" grade and was used as received following storage under nitrogen. All other materials were reagent grade and used as received. Potassium hydrotris(pyrazolyl)borate was synthesized according to the reported method, as was $[HB(pz)_3]VCl_2$·DMF.[20]

Synthesis. A. [LVCl{μ-(PhO)$_2$PO$_2$}]$_2$ (I). $[HB(pz)_3VCl_2$·DMF] (0.814 g, 2.0 mmol) and $Na[(C_6H_5O)_2PO_2]$ (0.544 g, 2.0 mmol) were mixed in a Schlenk flask, CH_3CN (30 mL) was added, and the mixture was brought rapidly to reflux temperature. The reaction mixture was stirred for 10−15 min producing a green solution. A light green precipitate formed as the solution cooled. After stirring for an additional 2 h, the precipitate was collected by filtration. The solid was dissolved in dry CH_2Cl_2 and filtered a second time to remove sodium chloride formed in the initial reaction. Crystals of complex **I** precipitate from the solution on standing at room temperature over 2 days. Higher yields of the product can be obtained by concentrating the CH_3CN from the initial reaction before collecting the precipitate, extracting with dry CH_2Cl_2, and then removing the CH_2Cl_2 under vacuum. Yield: 0.935 g (84%). Anal. Calcd for **I**·11/2 CH_2Cl_2: C, 43.50; H, 3.49; N, 13.53. Found: C, 43.10; H, 3.70; N, 13.69. IR (cm^{-1}): 2500, 1589, 1403, 1311, 715, 688, 658, 618. UV/vis, λ (ϵ): 422 nm (57), 606 nm (19).

B. [LVCl{μ-Ph$_2$PO$_2$}]$_2$ (II). $[HB(pz)_3VCl_2$·DMF] (0.814 g, 2.0 mmol) and $Na[(C_6H_5)_2PO_2]$ (0.480 g, 2.0 mmol) were mixed in a Schlenk flask. CH_3CN (30 mL) was added and the mixture brought rapidly to reflux temperature. The reaction mixture was cooled and stirred overnight producing a green solution and a light green precipitate. The precipitate was collected, and the desired product was separated from the NaCl, also formed in the reaction, by extraction with CH_2Cl_2. Crystals of complex **II** suitable for X-ray structure determination formed in the filtrate on standing over 3−4 days. Yield: 0.637 g (59%). Anal. Calcd for **II**·1/2 CH_2Cl_2: C, 47.46; H, 3.84; N, 15.63. Found: C, 47.44; H, 3.91; N, 15.50. IR (cm^{-1}): 2500, 1615, 1592, 1499, 1486, 1437, 1307, 662, 615, 559. UV/vis, λ (ϵ): 420 nm (140) 618 nm (56).

C. [LVCl{μ-PhP(H)O$_2$}]$_2$ (III). $[HB(pz)_3VCl_2$·DMF] (0.816 g, 2.0 mmol) and $Na[(C_6H_5)P(H)O_2]$ (0.328 g, 2.0 mmol) were mixed in a Schlenk flask. CH_3CN (40 mL) was added and the mixture brought rapidly to reflux temperature. The reaction mixture was stirred for 30 min producing a clear green solution and a light precipitate. The reaction mixture was filtered and the solid discarded. The CH_3CN filtrate was slowly concentrated under a stream of dry nitrogen gas, and a crop of very fine green needles, unsuitable for crystallography, was obtained. The crystals were collected by filtration and dried. Yield: 0.472 g (54%). Anal. Calcd for **III**·MeCN: C, 41.68; H, 3.83; N, 19.75. Found: C, 41.72; H, 3.84; N, 19.96. IR (cm^{-1}): 2500, 1499, 1433, 1403, 1304, 711, 695, 655, 622, 549. UV/vis, λ (ϵ): 424 nm (94) 600 nm (30).

D. [LV{(PhO)$_2$POS}$_2$DMF] (IV). $[HB(pz)_3VCl_2$·DMF] (0.407 g, 1.0 mmol) and $N(C_6H_{11})_4[(C_6H_5O)_2POS]$ (0.90 g, 2.0 mmol) were mixed in a Schlenk flask. CH_3CN (30 mL) was added and the mixture brought rapidly to reflux temperature. The reaction mixture was stirred for 10−15 min producing a pale green/blue solution. Cyclohexylammonium chloride formed in the reaction was removed by filtration. The filtrate volume was reduced under a flow of dry N_2, and the product

(18) Sakuai, H.; Tamura, H.; Okatami, K. *Biochem. Biophys. Res. Commun.* **1995**, *206*, 137. Otieno, T.; Bond, M. R.; Mokry, L. M.; Walters, R. B.; Carrano, C. J. *J. Chem. Soc., Chem. Commun.* **1996**, 37.
(19) See Trofimenko, S. *Chem. Rev.* **1972**, *72*, 497. Trofimenko, S. *Chem. Rev.* **1993**, *93*, 943. Maitlis, P. M. *Chem. Soc. Rev.* **1981**, 1.
(20) Mohan, M.; Holmes, S. M.; Butcher, R. J.; Jasinski, J. P.; Carrano, C. J. *Inorg. Chem.* **1992**, *31*, 2029.

was obtained as a light gray crystalline solid. Yield: 0.131 g (15%). Anal. Calcd for **IV**: C, 49.84; H, 4.30. Found: C, 50.04; H, 4.34. IR (cm^{-1}): 2500, 1651, 1593, 1405, 1312, 711, 687, 656, 618. UV/vis, λ (ϵ): 576 nm (17).

E. [LV{(PhO)$_2$PO$_2$}]$_2$·H$_2$O (V). [HB(pz)$_3$VCl$_2$·DMF] (0.407 g, 1.0 mmol) and Na[(C$_6$H$_5$O)$_2$PO$_2$] (0.544 g, 2.0 mmol) were mixed in a Schlenk flask. CH_3CN (30 mL) was added and the mixture brought rapidly to reflux temperature. The reaction mixture was stirred for 10−15 min, allowed to cool, and then filtered to remove NaCl formed in the reaction. Approximately 2 mL of degassed water was added to the filtrate, and the solution was allowed to stand at room temperature. Large dark crystals of complex **V** formed over 2−3 days. The complex was collected by filtration and dried. Yield: 0.304 g (39%). Anal. Calcd for **V**·CH_3CN: C, 51.18; H, 4.17; N, 11.94. Found: C, 51.04; H, 4.12; N, 11.84. IR (cm^{-1}): 2484, 1586, 1405, 1374, 1300, 711, 690, 663, 615. UV/vis, λ (ϵ): 438 nm (93), 640 nm (54).

X-ray Crystallography. Crystals of **I** and **V** were sealed in Lindemann glass capillaries and mounted on a Siemens P4 diffractometer at room temperature, while **II** and **IV** were glued to glass fibers and immediately transferred to the cold stream for data collection at 173 and 223 K, respectively. Unit cell constants were determined from least squares refinement of the angular settings of 25−35 well-centered, relatively high angle reflections. Data reduction, structure solution, and least squares refinement were done using the SHELXTL PLUS crystallographic software provided by Siemens.[21] Data collection, structure solution, and refinement parameters for each compound are summarized in Table 1. Details of the individual structure refinements are summarized below.

A. [LVCl(μ-(C$_6$H$_5$O)$_2$PO$_2$)]$_2$ (I). The structure solution was achieved by the Patterson method with anisotropic thermal parameters refined for all non-hydrogen atoms. The position of hydrogen atoms was calculated to give idealized geometries and then fixed to ride on their respective bound atoms with a fixed isotropic thermal parameter (0.08 Å^2). Final refinement of 316 least squares parameters against 1935 unique observed reflections ($F > 4.0\sigma(F)$) gave agreement factors $R = 4.99\%$ and $R_w = 5.74\%$ and excursions on the final difference map between +0.30 and −0.32 e Å^{-3}. Atomic coordinates are given in Table 2 with selected bond lengths and angles in Table 3.

B. [LVCl(μ-(C$_6$H$_5$)$_2$PO$_2$)]$_2$ (II). The presence of volatile dichloromethanes of crystallization necessitated low-temperature data collection. Structure solution and refinement proceeded normally, however, and were materially the same as those reported for **I**. Final refinement of 352 least squares parameters against 3043 unique observed reflections ($F > 4.0\sigma(F)$) gave agreement factors $R = 6.43\%$ and $R_w = 8.32\%$ and excursions on the final difference map between +1.30 and −0.68 e Å^{-3}. The largest difference peaks remaining were associated the ill-defined solvent molecules. Atomic coordinates are given in Table 4 with selected bond lengths and angles in Table 3.

C. [LV((C$_6$H$_5$O)$_2$PSO)$_2$(DMF)] (IV). The structure solution was again achieved through Patterson methods with other aspects of the solution and refinement as described for **I**. Final refinement of 505 least squares parameters against 2098 unique observed reflections ($F > 4.0\sigma(F)$) gave agreement factors $R = 5.97\%$ and $R_w = 6.40\%$ and excursions on the final difference map between +0.33 and −0.36 e Å^{-3}. Atomic coordinates are given in Table 5 with selected bond lengths and angles in Table 6.

D. [LV((C$_6$H$_5$O)$_2$PO$_2$)$_2$(H$_2$O)] (V). Data were collected at subambient temperature to prevent the loss of volatile acetonitriles of solvation. One acetonitrile of crystallization was reasonably well ordered and located on a general position; however, the nitrile carbon of a second was on a 2-fold axis giving rise to a 2-fold disorder between the methyl carbon and the nitrile nitrogen with a consequent averaging of the CN and CC bonds.

Final refinement of 500 least squares parameters against 3400 unique observed reflections ($F > 4.0\sigma(F)$) gave agreement factors $R = 3.86\%$ and $R_w = 4.82\%$ and excursions on the final difference map between +0.29 and −0.28 e Å^{-3}. Atomic coordinates are given in Table 7 with selected bond lengths and angles in Table 8.

(21) Sheldrick, G. M. *SHELXTL-PC*, Version 4.1; Siemans X-Ray Analytical Instruments, Inc.: Madison, WI, 1989. Scattering Factors from *International Tables for X-Ray Crystallography*; Ibers, J., Hamilton, W., Eds.; Kynoch: Birmingham, U.K., 1974; Vol. IV.

Table 2. Atomic Coordinates ($\times 10^4$) and Equivalent Isotropic Displacement Coefficients (Å^2 $\times$ 10^3) for **I**

	x	*y*	*z*	*U*(eq)[a]
V(1)	17(1)	1180(1)	3605(1)	26(1)
P(1)	1081(2)	1926(2)	6626(2)	30(1)
C1(1)	2312(2)	1364(2)	3442(2)	49(1)
O(1)	971(5)	1867(4)	5417(4)	34(2)
O(3)	921(6)	2888(4)	7107(4)	40(3)
N(5)	−2095(6)	1062(5)	3700(5)	28(3)
O(2)	−456(5)	−695(4)	3309(4)	37(3)
O(4)	2819(6)	2634(5)	7578(4)	47(3)
N(3)	−1193(6)	527(5)	1731(5)	32(3)
N(4)	−2229(7)	1022(5)	1328(5)	36(3)
N(1)	278(7)	3054(5)	3748(5)	35(3)
N(6)	−2982(6)	1549(6)	3081(5)	35(3)
N(2)	−894(7)	3264(5)	3092(5)	35(3)
C(3)	−442(11)	4511(8)	3276(8)	51(5)
C(6)	−2839(9)	422(8)	94(6)	48(4)
C(7)	−2849(8)	596(7)	4268(7)	41(4)
C(8)	−4202(9)	799(9)	4042(8)	56(5)
C(9)	−4248(8)	1394(8)	3298(7)	47(5)
C(5)	−2204(9)	−450(8)	−305(7)	50(4)
C(31)	−248(9)	2954(7)	8010(7)	36(4)
C(1)	1466(10)	4201(7)	4351(7)	46(4)
C(41)	3835(9)	3711(8)	7572(7)	47(5)
C(36)	−1749(11)	2720(9)	7714(8)	66(6)
C(35)	−2341(12)	2831(10)	8595(9)	79(7)
C(32)	718(11)	3352(8)	9218(7)	58(5)
C(4)	−1171(9)	−356(7)	738(7)	43(4)
C(2)	1047(12)	5140(8)	4074(8)	57(6)
B(1)	−2450(11)	2106(9)	2273(8)	41(5)
C(46)	4419(10)	3476(10)	6698(9)	66(5)
C(42)	4261(10)	4936(9)	8461(9)	6(5)
C(34)	−1352(13)	3218(9)	9799(9)	71(7)
C(33)	139(12)	3477(9)	10087(8)	66(6)
C(43)	5297(12)	5984(10)	8467(12)	91(8)
C(44)	5890(12)	5735(13)	7603(14)	102(9)
C(45)	5438(12)	4519(14)	6709(11)	93(8)

[a] Equivalent isotropic *U* defined as one-third of the trace of the orthogonalized U_{ij} tensor.

Table 3. Selected Bond Lengths (Å) and Angles (deg) for **I** and **II**

	I	**II**		**I**	**II**
V(1)−N1	2.084(7)	2.094(6)	V(1)−O1	1.983(5)	1.947(6)
V(1)−N3	2.083(6)	2.086(7)	V(1)−O2	2.003(5)	1.960(5)
V(1)−N5	2.112(7)	2.099(4)	V(1)−C1	2.316(3)	2.352(2)
C1−V(1)−O(1)	92.8(2)	92.0(1)	C1−V(1)−N(5)	177.2(2)	176.9(2)
O(1)−V(1)−N(5)	89.0(2)	88.6(2)	C1−V(1)−O(2)	91.3(2)	92.0(1)
O(1)−V(1)−O(2)	92.7(2)	94.90(2)	O(1)−V(1)−O(2)	173.2(3)	172.8(2)
C1−V(1)−N(3)	93.5(2)	93.6(1)	O(2)−V(1)−N(3)	89.7(2)	89.6(2)
N(5)−V(1)−N(3)	84.6(2)	85.6(2)	O(1)−V(1)−N(1)	92.4(2)	91.2(2)
C1−V(1)−N(1)	92.2(2)	91.9(1)	O(2)−N(1)−N(1)	173.7(2)	172.6(3)
N(5)−V(1)−N(1)	85.5(3)	85.0(2)	N(5)−V(1)−O(2)	90.7(2)	91.0(2)
N(3)−V(1)−N(1)	84.9(2)	83.0(3)			

Physical Measurements. Routine infrared spectra were obtained on a Perkin-Elmer 1600 FT-IR as KBr pellets. UV/vis spectra were recorded on an HP 8520 diode array spectrophotometer. Paramagnetic NMR spectra were obtained in $CDCl_3$ solution on a Bruker NR-80 80 MHz FT-NMR spectrometer. Electrochemical and magnetic susceptibility measurements were made as previously described.[22,23] All potentials are referenced versus the ferrocene/ferrocinum couple.

Results

Crystal Structure, Dimers. [LClV(μ-R)]$_2$: R = Diphenyl Phosphate (I), R = Diphenylphosphonate (II). These two V(III) complexes (Figures 1 and 2), which vary only in the nature of their bridging group, have many structural features in common with each other as well as with their vanadyl analogs. Both complexes have the V(III) ion in a pseudooctahedral

(22) Bonadies, J. A.; Carrano, C. J. *J. Am. Chem. Soc.* **1986**, *108*, 4088.
(23) O'Connor, C. J. *Prog. Inorg. Chem.* **1982**, *29*, 203.

Table 4. Atomic Coordinates ($\times 10^4$) and Equivalent Isotropic Displacement Coefficients ($Å^2 \times 10^3$) for **II**

	x	*y*	*z*	*U*(eq)[a]
V(1)	4640(1)	6119(1)	8266(1)	16(1)
Cl(2)	6858(2)	5152(2)	6798(1)	30(1)
P(1)	4487(2)	3582(1)	9618(1)	17(1)
O(1)	5416(4)	6165(4)	9316(3)	21(2)
O(2)	4610(4)	4509(4)	8716(3)	21(2)
B(1)	1966(8)	8489(7)	8073(7)	24(4)
N(1)	4437(5)	7901(4)	7757(4)	21(3)
N(2)	3183(5)	8817(4)	7767(4)	20(3)
C(1)	5281(7)	8432(6)	7464(5)	23(3)
C(2)	4615(8)	9682(6)	7291(6)	33(4)
C(3)	3287(8)	9890(6)	7485(6)	31(4)
N(3)	3613(5)	6294(4)	7229(4)	19(3)
N(4)	2487(5)	7385(4)	7254(4)	20(3)
C(4)	3803(7)	5505(6)	6481(5)	26(4)
C(5)	2798(7)	6085(6)	6011(6)	30(4)
C(6)	1994(7)	7268(7)	6534(6)	28(4)
N(5)	2648(5)	7074(4)	9535(4)	17(3)
N(6)	1617(5)	8047(4)	9293(4)	19(3)
C(7)	2079(6)	6925(5)	10647(5)	19(3)
C(8)	710(6)	7789(6)	11113(5)	24(3)
C(9)	456(6)	8480(6)	10240(6)	23(3)
C(31)	2825(7)	3573(5)	10076(5)	21(3)
C(32)	2476(7)	3304(6)	9279(6)	25(3)
C(33)	1204(8)	3300(7)	9614(6)	36(4)
C(34)	283(7)	3577(6)	10740(6)	32(4)
C(35)	616(7)	3859(6)	11536(6)	29(4)
C(36)	1901(7)	3849(6)	11197(5)	25(3)
C(41)	5804(6)	2072(5)	8924(5)	22(3)
C(42)	6561(8)	1943(7)	7776(6)	40(4)
C(43)	7533(9)	773(8)	7232(8)	59(5)
C(44)	7756(8)	−268(7)	7864(8)	51(5)
C(45)	7003(9)	−154(6)	9008(8)	48(5)
C(46)	6031(8)	1008(7)	9538(7)	43(4)
C(50)	−65(9)	12515(9)	5586(8)	64(5)
Cl(3)	579(3)	13228(3)	4403(2)	84(2)
Cl(4)	1108(3)	10976(2)	5641(2)	71(1)
C(51)	3515(9)	12493(8)	5273(7)	51(5)
Cl(5)	5115(2)	12151(2)	5296(2)	54(1)
Cl(6)	2132(2)	13201(2)	6581(2)	51(1)

[a] Equivalent isotropic *U* defined as one-third of the trace of the orthogonalized U_{ij} tensor.

environment with three coordination sites on the metal occupied by the tris(pyrazolyl)borate capping ligand. A chloride ion occupies the fourth, terminal site with the remaining two positions filled by the oxygen atoms of the bridging phosphate or phosphonate which serve to link two vanadiums together to form the dinuclear unit. Both **I** and **II** have inversion site symmetry which leads to the coordinated chloride ions adopting an "anti" arrangement with respect to each other and to only one-half the molecule being crystallographically unique. Finally, if one were to replace the "terminal" chloride with an oxo group, then these V(III) complexes are also effectively isostructural with their V(IV) or "vanadyl", counterparts.[4] So much so in fact that we have found yet another example of the phenomenon, previously referred to as "bond stretch" isomerization.[24−26] This phenomena is actually the result of a dilute solid solution of the V(III) chloro derivative in a vanadyl dimer host. This produces a material whose crystal structure (data not shown) is essentially identical to that reported in ref 4 but with a longer than expected oxo V(IV) bond due to the presence of an estimated ca. 7% of the V(III) chloro complex.

The overall conformation of the eight-membered $V(RPO_2)_2V$ ring is also surprisingly similar for the two molecules **I** and **II**.

Table 5. Atomic Coordinates ($\times 10^4$) and Equivalent Isotropic Displacement Coefficients ($Å^2 \times 10^3$) for **IV**

	x	*y*	*z*	*U*(eq)[a]
V(1)	474(2)	448(2)	2740(1)	37(1)
P(1)	1500(3)	3432(3)	2906(2)	39(2)
P(2)	−2681(3)	−396(3)	1836(2)	40(2)
S(1)	1183(3)	4277(3)	3857(2)	57(2)
S(2)	−3512(3)	−588(3)	2703(2)	56(2)
O(1)	−175(8)	863(7)	3732(5)	50(4)
O(2)	901(6)	2107(6)	2622(4)	39(3)
O(3)	1072(7)	4041(6)	2165(5)	39(4)
O(4)	3010(7)	3520(6)	2985(4)	44(4)
O(5)	−1234(7)	88(6)	2030(4)	42(4)
O(6)	−2926(7)	−1587(6)	1181(5)	50(4)
O(7)	−3287(7)	376(6)	1248(4)	43(3)
B(1)	2422(16)	−1211(14)	2695(11)	59(9)
N(1)	2296(9)	689(9)	3526(7)	44(5)
N(2)	3004(12)	−110(9)	3385(7)	52(6)
C(1)	2953(14)	1512(12)	4180(9)	54(7)
C(2)	4126(13)	1285(13)	4476(8)	59(7)
C(3)	4113(15)	253(15)	3959(11)	71(8)
N(3)	1271(10)	−108(9)	1800(7)	48(5)
N(4)	2144(11)	−784(9)	1897(8)	51(6)
C(4)	2565(14)	−939(12)	1227(12)	65(8)
C(5)	2001(16)	−374(14)	677(10)	70(8)
C(6)	1186(12)	115(11)	1069(11)	57(7)
N(5)	235(10)	−1323(8)	2884(6)	44(5)
N(6)	1155(10)	−1892(10)	2819(6)	56(6)
C(7)	748(16)	−3002(12)	2943(9)	73(8)
C(8)	−454(16)	−3117(12)	3086(9)	83(9)
C(9)	−731(13)	−2065(12)	3041(8)	59(7)
N(7)	−1444(11)	1748(10)	4368(8)	62(6)
C(10)	−861(13)	1609(12)	3794(9)	57(7)
C(11)	−1434(17)	988(16)	4950(10)	129(12)
C(12)	−2234(14)	2603(12)	4395(9)	101(9)
C(21)	92(14)	3864(11)	793(10)	62(7)
C(22)	−33(15)	3490(14)	−26(11)	72(8)
C(23)	807(19)	2908(12)	−290(10)	72(8)
C(24)	1800(17)	2996(12)	286(11)	69(8)
C(25)	1876(13)	3067(11)	1099(10)	54(7)
C(26)	1027(13)	3639(10)	1362(9)	41(6)
C(31)	4943(14)	4570(12)	3922(9)	72(7)
C(32)	5993(14)	5519(16)	4181(9)	77(8)
C(33)	6062(16)	6481(14)	3819(11)	82(9)
C(34)	5083(17)	6491(12)	3196(11)	80(9)
C(35)	4025(13)	5509(12)	2910(8)	64(7)
C(36)	3999(12)	4568(10)	3290(8)	41(6)
C(41)	−5093(14)	−2270(11)	370(8)	53(6)
C(42)	−6225(14)	−3171(14)	110(8)	75(8)
C(43)	−6324(16)	−4201(14)	391(10)	77(9)
C(44)	−5335(16)	−4354(12)	929(10)	86(8)
C(45)	−4195(13)	−3474(12)	1205(8)	66(7)
C(46)	−4112(12)	−2453(10)	925(8)	40(6)
C(51)	−4456(14)	1704(13)	1737(8)	70(8)
C(52)	−4495(13)	2834(15)	2080(9)	86(9)
C(53)	−3402(15)	3757(11)	2285(9)	74(8)
C(54)	−2260(12)	3533(12)	2145(8)	62(7)
C(55)	−2220(13)	2446(12)	1801(8)	54(7)
C(56)	−3317(33)	1532(10)	1608(7)	44(6)

[a] Equivalent isotropic *U* defined as one-third of the trace of the orthogonalized U_{ij} tensor.

In both cases the ring adopts a modestly "chair" like conformation with dihedral angles between the VO_2 and PO_2 planes of 159.8° and 159.5°, respectively. This compares with the ideal of 120° found in chair cyclohexane and 180° for a completely planar system. The values found in **I** and **II** indicate a ring conformation similar to that found in the V(IV) analog with the 3,5-dimethylpyrazolylborate capping ligand and a diphenyl phosphate bridge.[3] Another way of describing the similarity in conformation between **I** and **II** is to note that the vanadium centers are 0.476 Å above and below the mean plane described by P1, P1A, O1, O1A, O2, and O2A in **I** and 0.449 Å in **II**. There are, however, some notable discrepancies between the structures of **I** and **II**. The most obvious of these is the

(24) Yoon, K.; Parkin, G.; Hughes, D. L.; Leigh, G. J. *J. Chem. Soc., Dalton Trans.* **1992**, 769.
(25) Yoon, K.; Parkin, G. *Inorg. Chem.* **1992**, *31*, 1656.
(26) Yoon, K.; Parkin, G.; Rheingold, A. L. *J. Am. Chem. Soc.* **1992**, *114*, 2210.

Table 6. Bond Lengths (Å) and Angles (deg) for **IV**

V(1)−O(1)	2.011(9)	V(1)−O(2)	1.965(7)
V(1)−O(5)	1.938(7)	V(1)−N(1)	2.109(10)
V(1)−N(3)	2.077(13)	V(1)−N(5)	2.110(10)
P(1)−S(1)	1.917(5)	P(1)−O(2)	1.520(7)
P(1)−O(3)	1.593(10)	P(1)−O(4)	1.618(8)
P(2)−S(2)	1.916(6)	P(2)−O(5)	1.518(7)
P(2)−O(6)	1.597(8)	P(2)−O(7)	1.601(9)
O(1)−V(1)−O(2)	92.1(3)	O(1)−V(1)−O(5)	92.0(3)
O(2)−V(1)−O(5)	93.6(3)	O(1)−V(1)−N(1)	87.8(4)
O(2)−V(1)−N(1)	91.3(4)	O(5)−V(1)−N(1)	175.1(4)
O(1)−V(1)−N(3)	172.7(4)	O(2)−V(1)−N(3)	92.9(4)
O(5)−V(1)−N(3)	93.0(4)	N(1)−V(1)−N(3)	86.7(4)
O(1)−V(1)−N(5)	90.9(4)	O(2)−V(1)−N(5)	173.6(4)
O(5)−V(1)−N(5)	91.9(3)	N(1)−V(1)−N(5)	83.2(4)
N(3)−V(1)−N(5)	83.6(4)	S(1)−P(1)−O(2)	120.1(4)
S(1)−P(1)−O(3)	108.2(4)	O(2)−P(1)−O(3)	107.3(4)
S(1)−P(1)−O(4)	112.8(3)	O(2)−P(1)−O(4)	102.2(4)
O(3)−P(1)−O(4)	105.3(5)	S(2)−P(2)−O(5)	119.6(4)
S(2)−P(2)−O(6)	114.2(4)	O(5)−P(2)−O(6)	102.7(4)
S(2)−P(2)−O(7)	112.5(4)	O(5)−P(2)−O(7)	106.6(4)
O(6)−P(2)−O(7)	98.8(4)		

difference in V···V distances, 5.21 Å in **I** versus 5.09 Å in **II**. Unlike the V(IV) analogs, this increase in distance cannot be attributed to a change in the conformation of the bridging ring which is, as described above, nearly equivalent for both complexes. Rather it is due to a difference in bond lengths between the vanadium and the bridging phosphate versus phosphonate oxygens. In **I** the V−O bonds are 1.983 and 2.003 Å while the corresponding distances in **II** are 1.947 and 1.960 Å. Thus the V−O bonds are an average 0.04 Å longer in the phosphate derivative leading directly to the increased V···V distance. It should be noted, however, that since the two structures were not determined at the same temperature strict bond length comparisons may not be valid.

Crystal Structures, Monomers. The structure of **IV** (Figure 3) shows the V(III) ion to be in a distorted octahedral environment with a facially coordinating tris(pyrazolyl)borate, two O-bonded unidentate monothiophosphate groups, and a coordinated DMF. The vanadium phosphate oxygen bonds average 1.951 Å, a value which is nearly exactly the same as those seen in the phosphonate (**II**), but shorter than those found in the phosphate-bridged dimer. There are no close intermolecular contacts, and other bond lengths and angles are unexceptional. The structure of **V** (Figure 4) is similar to that of **IV** in that the V(III) is coordinated by a tris(pyrazolyl)borate capping ligand, the oxygens of two unidentate diphenyl phosphates, and a water molecule. Bond lengths and angles are also quite similar. The major difference lies in the fact that in **V** there is very strong *intermolecular* hydrogen bonding between the hydrogens of the bound water on one molecule and the nonester phosphoryl oxygens on another which leads to the formation of dimeric units with a V···V distance of 5.92 Å. The average oxygen−oxygen contact in the V−OH···O−P unit is 2.64(1) Å with an angle near 160°, both of which suggest a strong hydrogen bond.

Characterization. A. Electrochemistry. Mononuclear complex **IV** showed no reversible electrochemistry at all while complex **V** gave a single poorly reversible oxidation wave at +1.02 V, a quasireversible reductive wave at −1.07 V, and another irreversible reductive wave at −1.55 V. On the basis of peak heights all these waves appeared to be one-electron processes. The electrochemical response of dinuclear complex **I** was similar to that of **V**; however, two closely spaced oxidative waves were also observed. The first of these (+1.025 V) was quasireversible with the second (P_c = 1.45 V), very near the edge of the solvent window, irreversible. Upon scanning in the reductive region the reversible reduction near −1.07 V was absent but an irreversible wave was evident near −1.575 V.

Table 7. Atomic Coordinates ($\times 10^4$) and Equivalent Isotropic Displacement Coefficients ($Å^2 \times 10^3$) for **V**

	x	*y*	*z*	*U*(eq)[a]
V(1)	38(1)	−854(1)	4176(1)	25(1)
O(1W)	836(2)	−261(1)	4524(1)	34(1)
P(1)	−786(1)	−1082(1)	5520(1)	30(1)
O(1)	−682(2)	−1054(1)	4884(1)	36(1)
O(2)	−369(2)	−662(1)	5879(1)	36(1)
O(3)	−215(2)	−1583(1)	5759(1)	38(1)
O(4)	−2049(2)	−1177(1)	5596(1)	34(1)
P(2)	−2164(1)	−154(1)	4105(1)	28(1)
O(5)	−1101(2)	−372(1)	3940(1)	32(1)
O(6)	−2287(2)	90(1)	4666(1)	35(1)
O(7)	−2521(2)	220(1)	3603(1)	39(1)
O(8)	−2962(2)	−622(1)	4007(1)	43(1)
B(1)	1103(4)	−1675(2)	3338(2)	39(1)
N(1)	−705(2)	−1469(1)	3748(1)	29(1)
N(2)	−108(3)	−1792(1)	3427(1)	34(1)
C(1)	−1706(3)	−1657(1)	3752(2)	33(1)
C(2)	−1764(3)	−2100(2)	3435(2)	42(1)
C(3)	−737(3)	−2174(2)	3237(2)	39(1)
N(3)	1318(2)	−1350(1)	4352(1)	31(1)
N(4)	1664(3)	−1672(1)	3932(1)	34(1)
C(4)	1948(3)	−1436(2)	4814(2)	38(1)
C(5)	2703(3)	−1807(2)	4702(2)	48(1)
C(6)	2498(3)	−1947(2)	4148(2)	47(1)
N(5)	812(2)	−732(1)	3408(1)	28(1)
N(6)	1175(2)	−1131(2)	3091(1)	32(1)
C(7)	1027(3)	−310(2)	3109(2)	33(1)
C(8)	1517(3)	−435(2)	2597(2)	41(1)
C(9)	1595(3)	−956(2)	2604(2)	40(1)
C(11)	−255(3)	−2450(2)	5995(2)	46(1)
C(12)	−466(4)	−2954(2)	5854(2)	58(1)
C(13)	−847(4)	−3086(2)	5323(2)	54(1)
C(14)	−1015(5)	−2721(2)	4931(2)	82(2)
C(15)	−804(5)	−2213(2)	5060(2)	80(2)
C(16)	−445(3)	−2081(1)	5594(2)	34(1)
C(21)	−2496(3)	−1553(2)	6497(2)	44(1)
C(22)	−2972(4)	−1514(2)	7034(2)	55(1)
C(23)	−3422(4)	−1071(2)	7202(2)	54(1)
C(24)	−3404(4)	−653(2)	6848(2)	56(1)
C(25)	−2939(3)	−685(2)	6308(2)	45(1)
C(26)	−2492(3)	−1135(2)	6145(2)	33(1)
C(31)	−2166(3)	1109(2)	3641(2)	42(1)
C(32)	−2542(4)	1602(2)	3688(2)	52(1)
C(33)	−3608(4)	1697(2)	3788(2)	53(1)
C(34)	−4313(3)	1300(2)	3850(2)	48(1)
C(35)	−3950(3)	805(2)	3802(2)	39(1)
C(36)	−2882(3)	717(2)	3695(2)	32(1)
C(41)	−4640(3)	−542(1)	4509(2)	42(1)
C(42)	−5759(4)	−553(2)	4491(2)	52(1)
C(43)	−6296(4)	−620(2)	3980(3)	58(1)
C(44)	−5749(4)	−677(2)	3480(2)	59(1)
C(45)	−4627(3)	−661(2)	3488(2)	48(1)
C(46)	−4090(3)	−594(1)	4007(2)	32(1)
N(7)[b]	0	1901(3)	2500	177(2)
C(51)[b]	0	1476(4)	1500	95(2)
C(52)[b]	0	949(3)	2500	158(2)
N(8)	5990(7)	1896(5)	7399(4)	240(2)
C(53)[b]	5000	1844(4)	7500	216(2)

[a] Equivalent isotropic *U* defined as one-third of the trace of the orthogonalized U_{ij} tensor. [b] Site occupation factors for N(7), C(51), C(52), and C(53) are 0.500.

Thus, this dinuclear complex shows the expected two sequential one-electron oxidations of V(III) to V(IV). These are not expected to be highly reversible, however, since the initial oxidations produce non-oxo V(IV) centers which are extremely oxophilic and react in a follow up process with traces of water in the solvent to yield V═O units. Similar behavior was seen with tetranuclear V(III) phosphato-bridged clusters previously reported.[2] Complex **II** shows an electrochemical response similar to that of **I,** but only the first oxidation wave is observed at +1.0 V, the second wave is lost in the rising solvent background.

B. Paramagnetic NMR. Due to the favorable electron relaxation properties of the V(III) ion, well-defined paramagnetic

Table 8. Bond Lengths (Å) and Angles (deg) for **V**

V(1)−O(1W)	2.010(2)	V(1)−O(1)	1.960(3)
V(1)−O(5)	1.967(2)	V(1)−N(1)	2.103(3)
V(1)−N(3)	2.085(3)	V(1)−N(5)	2.069(3)
O(1W)−H(1WA)	0.756(3)	O(1W)−H(2WA)	0.773(3)
H(1WA)−O(6A)	1.870(3)	H(2WA)−O(2A)	1.925(3)
P(1)−O(1)	1.489(3)	P(1)−O(2)	1.473(3)
P(1)−O(3)	1.591(3)	P(1)−O(4)	1.594(3)
O(1W)−V(1)−O(1)	95.6(1)	O(1W)−V(1)−O(5)	87.2(1)
O(1)−V(1)−O(5)	94.1(1)	O(1W)−V(1)−N(1)	174.9(1)
O(1)−V(1)−N(1)	89.4(1)	O(5)−V(1)−N(1)	93.6(1)
O(1W)−V(1)−N(3)	92.5(1)	O(1)−V(1)−N(3)	91.3(1)
O(5)−V(1)−N(3)	174.5(1)	N(1)−V(1)−N(3)	86.1(1)
O(1W)−V(1)−N(5)	89.7(1)	O(1)−V(1)−N(5)	173.4(1)
O(5)−V(1)−N(5)	90.0(1)	N(1)−V(1)−N(5)	85.2(1)
N(3)−V(1)−N(5)	84.5(1)	H(1WA)−O(1W)−H(2WA)	111.9(1)
O(1W)−H(1WA)−O(6A)	166.6(1)	O(1W)−H(2WA)−O(2A)	160.9(1)
O(1)−P(1)−O(2)	119.2(2)	O(1)−P(1)−O(3)	110.0(1)
O(2)−P(1)−O(3)	106.2(1)	O(1)−P(1)−O(4)	102.9(1)
O(2)−P(1)−O(4)	112.7(1)	O(3)−P(1)−O(4)	105.0(1)

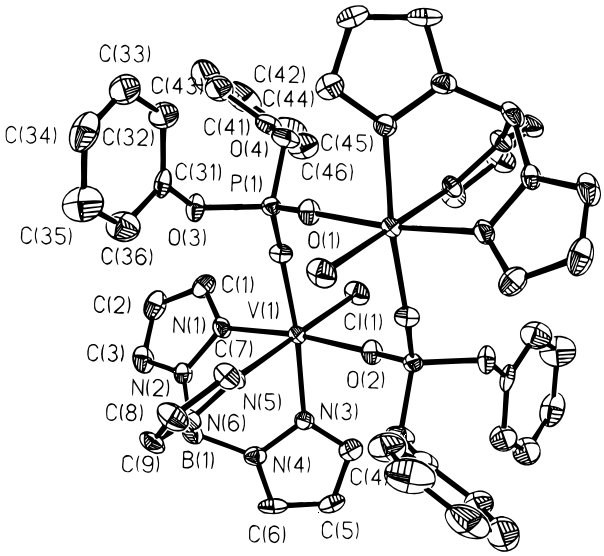

Figure 1. Thermal ellipsoid plot (30%) of **I** showing the atom labeling scheme.

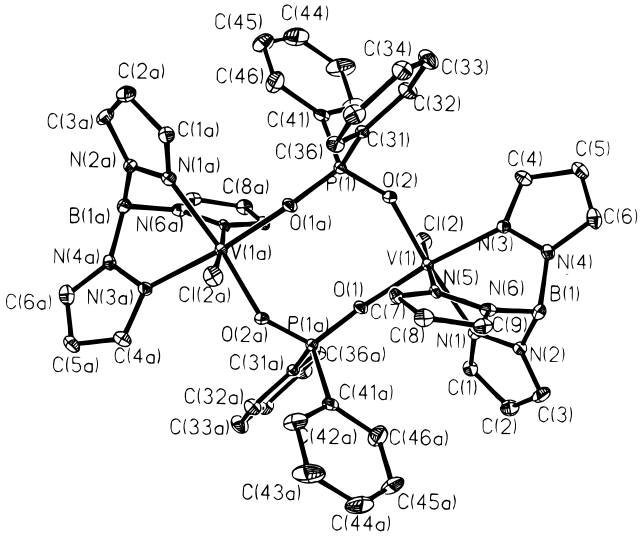

Figure 2. Thermal ellipsoid plot (30%) showing the atom labeling scheme for **II**.

NMR spectra were obtained on several compounds prepared in this study. The assignments were made on the basis of our previous experience with analogous oxo- and hydroxo-bridged V(III) complexes.[27] The spectra reflect the overall symmetry

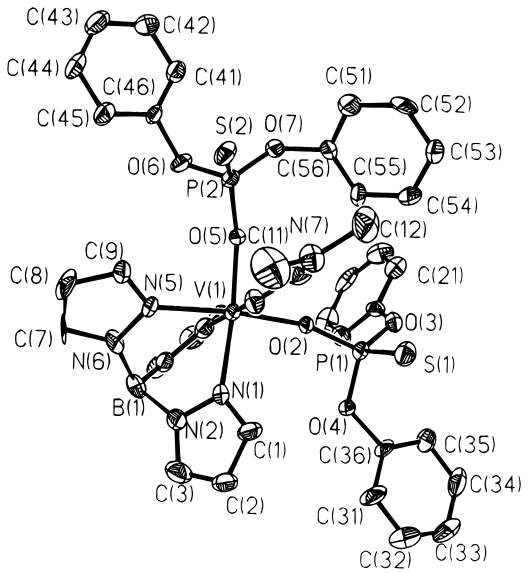

Figure 3. Thermal ellipsoid plot (30%) showing the atom labeling scheme for **IV**.

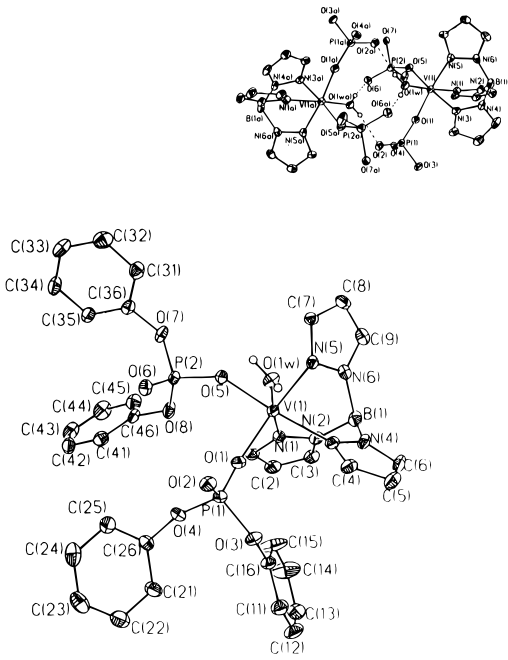

Figure 4. Thermal ellipsoid plot (30%) of **V** showing the atom labeling scheme. The insert shows the hydrogen-bonded dimer.

of the complexes in question, i.e., 3-fold symmetric complexes of the type $[LV(diphenyl\ phosphate)_3]_2Mg$ (data not shown) show only one set of resonances each for the 3, 4, and 5 position pyrazole protons, while complexes with a plane of symmetry, i.e., **I** and **II** show two sets of resonances indicative of "cis" and "trans" orientations of these protons relative to the terminal chloride. Finally, complexes completely lacking a plane of symmetry should show separate resonances for each of the protons on each pyrazole ring of the tris(pyrazolyl)borate. From this we can deduce for example that the monophenylphosphinate dimer **III** (for which no crystal structure is available) must adopt an "anti" structure for the bridge phenyl rings. This removes the plane of symmetry, and hence separate resonances are observed for each proton on each pyrazole ring of the tris(pyrazolyl)borate.

As noted above, in dimers **I** and **II** the 3, 4, and 5 pyrazole protons (Figure 5) appear in two groups with a 2:1 ratio

(27) Bond, M. R.; Czernuszewicz, R. S.; Dave, B. C.; Mohan, M.; Verastgue, R.; Carrano, C. J. *Inorg. Chem.* **1995**, *34*, 1233.

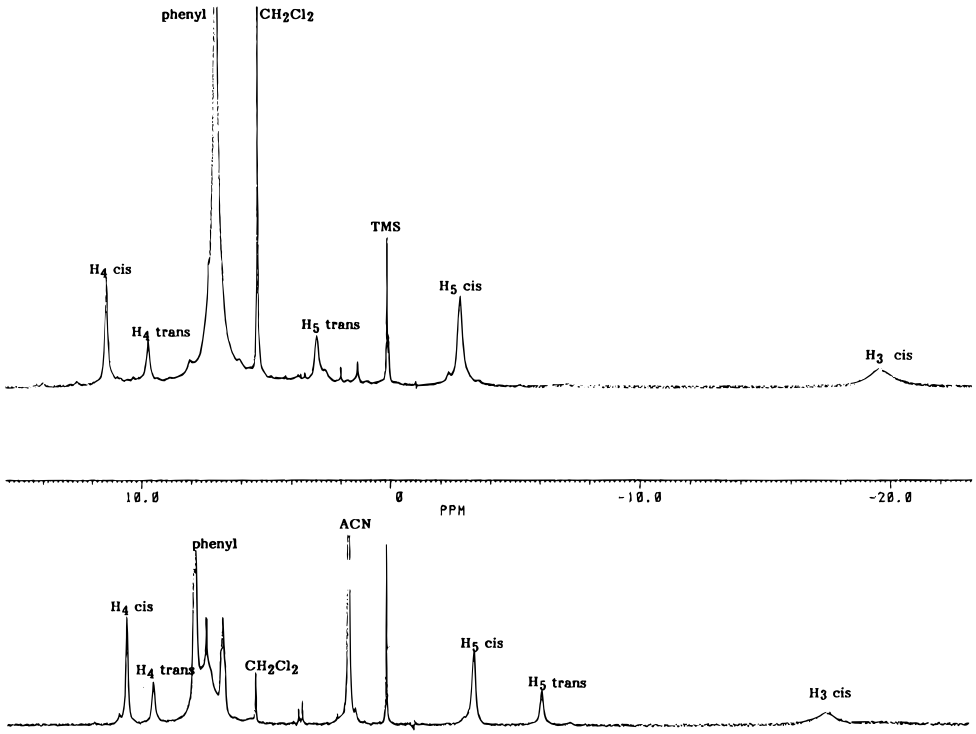

Figure 5. Paramagnetic NMR spectra of **I** (top) and **II** (bottom) in $CDCl_3$.

corresponding to the two pyrazole rings "cis" to the terminal chloride and the one ring "trans" to it. In both complexes the cis pyrazole protons follow an alternating sign pattern around the ring with the 3 and 5 protons experiencing an upfield shift and the 4 proton a downfield one. This is consistent with a π delocalization mechanism for the transfer of the unpaired spin density from V(III) onto the ligand. However, the two complexes differ in the behavior of the trans protons. While in **II** the trans protons also follow the alternating sign pattern shown for the cis protons, in **I** the H5 trans proton undergoes a large downfield shift relative to **II** such that the alternating sign pattern is lost. This is analogous to what happens upon protonation of the oxo bridge in the (μ-oxo{hydroxo})bis(μ-diphenylphosphato)divanadium(III) pair of complexes previously reported and has been interpreted to indicate a change in the delocalization pathway from π to σ.[27] This shift is accompanied in the latter example by a change in magnetic properties from strongly ferromagnetically coupled (oxo complex with π pathway) to antiferromagnetically coupled (hydroxo bridged with σ path). We can also interpret the large downfield shift of H5 in the phosphate versus phosphonate dimer in the present case to a change in delocalization pathway. This would presumably arise from a change in orbital occupancy which in turn could be explained by the dramatic increase in either ZFS or antiferromagnetic coupling on going from **II** to **I**.

C. Magnetic Measurements. Variable temperature magnetic susceptibility data were collected in the temperature range 1−250 K for both **I** and **II**. An empirical diamagnetic correction was derived for each from a plot of susceptibility versus inverse temperature and applied to the data. The effective moment of the phosphonate-bridged dimer **II** remains essentially constant throughout most of the temperature range before decreasing at very low temperature, but no maximum in the susceptibility is observed. Fits of the data to either an $S = 1$ HDVV (Heisenberg−Dirac−Van Vleck) dimer model or a zero field splitting (ZFS) model[28] were unsatisfactory, but a fit of the data to simple Curie−Weiss behavior was successful with $C = 1.53(1)$ emu·K/mol, and $\Theta = -4.41(9)$ K, Figure 6. The low-temperature behavior of the effective moment probably arises from several distinct interactions including intra- and interdimer exchange and single ion ZFS which are of similar magnitudes and cannot be adequately modeled by just one interaction. In any event the magnitude of these interactions is quite small no matter what their exact origin. In contrast the χ versus T plot of the data from **I** shows a distinct maximum around 6 K indicating substantially stronger antiferromagnetic interactions than in **II**. Nevertheless, a least squares fit to an $S = 1$ HDVV dimer model with Curie−Weiss and impurity corrections yielded only fair results and gave unrealistically high values for both the Weiss constant and the impurity correction. A least squares fit to a ZFS model with Curie−Weiss and impurity corrections gave considerably better results with parameters $g = 1.688(1)$, $D/k = 18.1(4)$ K, $\Theta = -14.2(1)$ K, and a 3.8(2)% paramagnetic impurity (Figure 7). It should be noted, however, that a Θ term in the ZFS model has no real physical significance and that a better way to model a weak secondary interaction is to apply

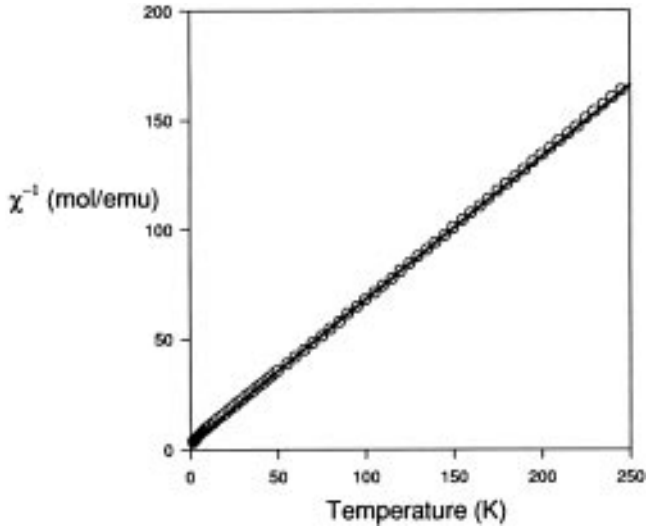

Figure 6. Curie−Weiss plot for **II**. The solid line represents the linear least squares fit using the parameters in the text, and the open circles represent the data.

(28) Carlin, R. L. *Magnetochemistry*; Springer-Verlag: Berlin, 1986; p 24.

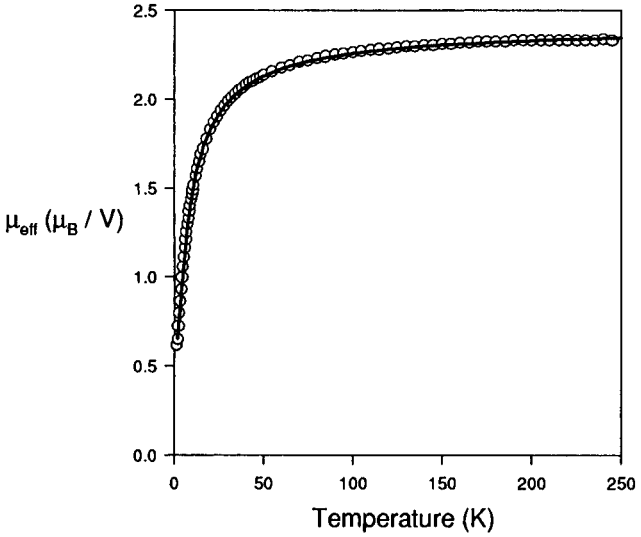

Figure 7. Plot of μ_{eff} vs T for **I**. The solid line represents the nonlinear least square fit to the data using the model and parameters given in the text.

the molecular field (MF) approximation.[23] Using this approach an equally good fit to the data can be obtained to give g = 1.694(1), D/k = 27.1(3) K, and zJ'/k = −4.51 K where z = the number of exchange coupled neighbors and J' the exchange coupling constant. Applying the MF approximation to the HDVV model also gave a good fit to the data with J/k = −4.56(5) K, g = 1.681(9), zJ'/k = −2.56(4) K, and a 4.1% paramagnetic impurity correction. The norms for the two fits are comparable although there is one more parameter employed in the exchange-coupled model.

Discussion

The di-μ-phosphato-bridged dinuclear unit found in several of the these V(III) complexes has previously been found for the Cu(II), Ni(II), and Cd(II) complexes of various nucleotides[29−31] and also represents a common structural motif in numerous V(III) and V(IV) phosphate solid state materials. Despite the stability of the phosphato-bridged dinuclear unit, unidentate phosphate-coordinated mononuclear complexes can also be isolated, and their formation seems to be largely a matter of stoichiometry rather than inherent stability. However, the strict formation of only O-bonded mononuclear complexes when monothiophosphate was used as a ligand illustrates a surprisingly strong preference of V(III) for the harder O over the softer S donor given the relatively large number of known V(III)−S complexes.[32,33] The structure of **V** shows that the interaction of V(III) complexes with phosphates can occur by both inner and outer sphere processes. The very strong hydrogen bonding between the nonester phosphorus oxygens and the coordinated water molecule is reminiscent of the mode of interaction of Cp_2VCl_2 with diphenyl phosphate.[13] However, hydrolysis of Cp_2VCl_2 produces two bound water molecules per vanadium center and leads to a hydrogen-bonded infinite chain rather than the discrete dimers as seen in **V**. Other examples of outer sphere metal nucleotide/DNA phosphate complexation are also known.[34]

Of particular interest to us is the ability of the phosphate group or its analogs to transmit magnetic interactions between metal centers in simple dinuclear molecules. This has important ramifications to understanding magnetic interactions in more complex solid state vanadium phosphates. We have already shown that the conformation of the $V(OPO)_2V$ unit strongly affects both the magnitude and the type of magnetic interaction in V(IV) phosphates.[4] It was therefore surprising that **I** and **II**, which have such similar structures in general and $V(OPO)_2V$ conformations in particular, display quite different magnetic properties. The latter shows essentially no interaction while the V(III) centers in the former do. Unfortunately, while in the vanadyl dimers there is just a single unpaired electron/vanadium in a well-defined orbital making it relatively easy to identify an exchange pathway, in the V(III) systems the possible presence of intradimer exchange and ZFS cloud the picture. This is so since, phenomenologically, ZFS can give rise to magnetic behavior that is difficult to distinguish from *intra*- or *inter*dimer antiferromagnetic exchange coupling. In the ZFS model the value of D obtained for **I** is both reasonable in magnitude and of the same sign as all other known examples of V(III).[28] We interpret the zJ'/k term of −4.41 K in the molecular field corrected ZFS model as a measure of either or both intra- or interdimer antiferromagnetic coupling. The fact that J/k in the exchange-coupled model for **I** and zJ'/k in the ZFS one are both on the order of −4 K suggests that the latter in fact represents intradimer antiferromagnetic coupling. In the HDVV model zJ'/k probably represents a weak interdimer exchange which is also antiferromagnetic. It would be somewhat surprising if any *intra*dimer AFC present should be larger in **I** versus **II** given that the phosphonate dimer **II** actually has the shorter V···V distance hence it may be that the *inter*dimer coupling is most important in this system. The packing diagram shows that both complexes pack essentially in layers with the interlayer distance dependent on the presence or absence of the solvent of crystallization. Thus interdimer coupling should be greatest for **I** with no solvent and consequent closer layer packing as compared to **II** which has its layers separated by dichloromethanes and hence farther apart. Alternatively the magnetic differences between **I** and **II** may arise from electronic differences between the phosphate versus phosphonate bridging ligands. A definitive answer, however, will require more detailed field-dependent and/or single crystal magnetic measurements which will hopefully be forthcoming.

Acknowledgment. C.J.C. wishes to thank the Robert A. Welch foundation through Grant AI-1157 and the NIH through AREA Grant GM4767601 for partial support of this work. The NSF-ILI program Grant USE-9151286 is also acknowledged for support of the X-ray diffraction facilities at SWTSU.

Supporting Information Available: Complete lists of atomic positions, bond lengths and angles, anisotropic displacement parameters, hydrogen atom coordinates, and data collection and crystal structure parameters for **I**, **II**, **IV**, and **V**, as well as χ versus T plots for **I** and **II** (37 pages). Ordering information is given on any current masthead page.

IC9514556

(29) Fischer, B. E.; Bau, R. *Inorg. Chem*. **1978**, *17*, 27.
(30) Aoki, K. *J. Chem. Soc., Chem. Commun*. **1979**, 589.
(31) Wei, C.; Fischer, B. E.; Bau, R. *J. Chem. Soc., Chem. Commun*. **1978**, 1053.
(32) Wiggens, R. W.; Huffman, J. C.; Christou, G. *J. Chem. Soc., Chem. Commun*. **1983**, 1314.
(33) Heinrich, D. D.; Folting, K.; Huffman, J. C.; Reynolds, J. G.; Christou, G. *Inorg. Chem*. **1991**, *30*, 300.
(34) Gessner, R. V.; Quigley, G. J.; Wang, A. H.; van der Marel, G. A.; van Boom, J. H.; Rich, A. *Biochemistry* **1985**, *24*, 237.